Electronic structure of $Bi_2Sr_2Ca_{1-x}Y_xCu_2O_{8+\delta}$: Cu 2p x-ray-photoelectron spectra and occupied and unoccupied low-energy states

M. A. van Veenendaal and G. A. Sawatzky
Laboratory of Applied and Solid State Physics, Materials Science Centre, University of Groningen, Nijenborgh 4, 9747 AG Groningen, The Netherlands

W. A. Groen
Philips Research Laboratories, P.O. Box 80000, 5600 JA Eindhoven, The Netherlands
(Received 8 July 1993)

In this paper we will present measurements, using various kinds of spectroscopy, on the hole-doped compound $Bi_2Sr_2Ca_{1-x}Y_xCu_2O_{8+\delta}$, with x ranging from 0.0 to 1.0. Cu 2p x-ray photoelectron spectra are compared with cluster calculations using nonlocal screening effects. The consequences of hole doping and multiplet interaction are also studied. The photoemission and inverse-photoemission data indicate that the appearance of intensity at the Fermi level is a result of the shift of the chemical potential to the top of the valence band combined with a shift of spectral weight from high- to low-energy states.

I. INTRODUCTION

During recent years it has become quite generally accepted that the insulating nature of the parent compounds of the high-temperature oxide superconductors can only be understood by taking into account the strong correlations between electrons. The gap is known to be of a charge-transfer-like nature,[1] where the lowest-energy electron removal states have mainly oxygen character, the so-called Zhang-Rice singlets.[2,3] In this paper we will show that these states are not only relevant for valence-band photoemission spectroscopy, but are also of crucial importance for understanding the Cu 2p x-ray photoelectron spectrum (XPS). This is not only the hole-doped compounds, but also for the insulators.

Despite the general consensus on the insulators, the doped systems still generate a lot of controversy. The question remains whether the strong correlations, so apparent in the parent compounds, lead to a breakdown of the Fermi-liquid-like picture or whether the doped holes (electrons) cause a collapse of the strong interactions and lead to a, albeit renormalized, bandlike picture. We will address these points when comparing our photoemission (PES) and inverse photoemission (IPES) data on the $Bi_2Sr_2Ca_{1-x}Y_xCu_2O_{8+\delta}$ series with model calculations.

The paper is divided as follows. We will start with a description of the experimental technique and the sample preparation. The remainder of the paper is divided into two parts. The first part provides a detailed description of the Cu 2p XPS line shape. In the second part we will discuss the behavior of the occupied and unoccupied states near the Fermi level as a function of doping.

II. EXPERIMENTAL

The $Bi_2Sr_2Ca_{1-x}Y_xCu_2O_{8+\delta}$ have been prepared by a spray drying technique to obtain a maximum homogeneity, as was described earlier.[4] The samples were carefully checked for deviations from the expected stoichiometry by iodometry and inductive coupled plasma analysis to determine the copper content and the copper-to-bismuth ratio, respectively. The formal copper valency was determined via the oxidizing power by means of chemical titration. Holes can be induced into the CuO_2 planes by replacing trivalent yttrium by divalent calcium in the antiferromagnetic insulator $Bi_2Sr_2YCu_2O_{8.51}$. The samples with a higher yttrium percentage also contained more oxygen. The extra oxygen is probably incorporated in the Bi_2O_2 planes.

The metal-insulator transition for these compounds lies somewhere around $x=0.6$, which corresponds to a hole density of approximately 0.06 holes per CuO_2 unit.[4] The metallic compounds also show superconductivity. The maximum critical temperature for these compounds, and also for a number of other Bi-based high-T_c superconductors,[4] is reached for a hole density of 0.15–0.17 holes per CuO_2 unit. Some characteristics of the samples used in this study are tabulated in Table I.

TABLE I. Several characteristics of the $Bi_2Sr_2Ca_{1-x}Y_xCu_2O_{8+\delta}$ samples. For the different values of Yttrium doping (x), the oxygen content (δ), the number of holes per CuO_2 unit, the critical temperature, and the shift needed to match the leading edge of the valence band for the XPS are given (see also Refs. 4 and 6).

x	δ	Holes per CuO_2 unit	T_c (K)	Fermi level shift XPS (eV)
0.00	0.23	0.23	70	0
0.10	0.23	0.18	85	0.03
0.30	0.30	0.15	86	0.04
0.40	0.29	0.09	64	0.12
0.50	0.33	0.08	40	0.15
0.75	0.41	0.03	<4	0.41
1.00	0.51	0.01	<4	0.64

The XPS data have been measured by a "top hat" X-probe 300 from Surface Science Instruments. The radiation source is a monochromatized Al $K\alpha$ line ($\hbar\omega = 1486.6$ eV). When using a 600 μm spot size the overall resolution is 1 eV. The low-energy photoemission and inverse-photoemission spectra were measured in a different instrument. The ultraviolet photoemission spectroscopy (UPS) spectra were taken using a He I resonance line ($\hbar\omega = 21.2$ eV). The inverse-photoemission (IPES) spectrometer makes use of a grating, which disperses the emitted photons onto a position-sensitive detector. The IPES system was built in our group and follows a design by Johnson *et al.*[5] To minimize the effects of charging, low sample currents of 2.5 μA were used. However, for insulating compounds, charging effects are almost unavoidable. As a result of the low cross section of inverse photoemission (about 10^{-4} times lower than photoemission) much higher electron currents are needed compared to PES. The resolution is 100 meV for UPS. For IPES the resolution is 300 meV for low photon energies, where the resolution is mainly determined by the energy spread of the electron gun. At higher photon energies the energy resolution of the grating deteriorates and becomes the dominating effect for the resolution. At photon energies higher than 25 eV the resolution is 1 eV.

The $Bi_2Sr_2Ca_{1-x}Y_xCu_2O_{8+\delta}$ samples were cleaned by scraping them in vacuum with a diamond file. This resulted in surfaces on which no traces of contamination were found, i.e., no signal of the C 1*s* level and no shoulders on the high binding energy side of the O 1*s* peak. The pressure in both systems was in the low 10^{-10} Torr regime.

III. Cu 2*p* XPS CORE-LEVEL LINE SHAPES

First we shall discuss the shape of the Cu 2*p* XPS line shape. In the description of the Cu 2*p* core line (see Fig. 1) there are a number of points that have remained unclear (for more details on the XPS data see Ref. 6). First of all, there is the wide asymmetric shape of the main line. So far this has been interpreted in terms of oxygen band effects, resulting from the expected mainly $\underline{c}3d^{10}\underline{L}$ character of the main line[7] (where $\underline{c}$ and $\underline{L}$ stand for a core and a ligand hole, respectively). Anderson impurity calculations, however, show this peak to be skewed towards the top of the oxygen band. Also, the assumption that the width is a result of the oxygen band leads to the problem of why $NaCuO_2$ has a narrow main line[8,9] whereas its character should be of $\underline{c}3d^{10}\underline{L}^2$. Second, the Cu 2*p* core line consistently gives low estimations of the value of the charge-transfer energy when comparing model parameters obtained from valence band[10] and Cu 2*p* photoelectron spectroscopy.[11,12] Third, the question of doping still remains unclear. Is it, e.g., possible to describe the hole-doped spectrum by a simple superposition of a spectrum of the insulating compound and a spectrum of a 100% doped sample (cf., for example $NaCuO_2$).

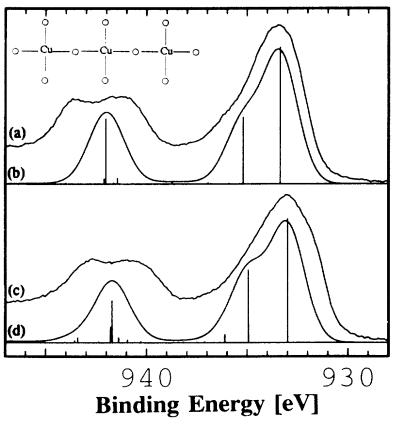

FIG. 1. Comparison of calculated and experimental Cu 2*p* spectra. From top to bottom (a) Cu $2p^{3/2}$ spectrum of $Bi_2Sr_2YCuO_{8.51}$ (0.01 holes per CuO_4 unit), (b) calculated Cu 2*p* spectrum for the Cu_3O_{10} cluster (see inset) with three holes, (c) Cu $2p^{3/2}$ of $Bi_2Sr_2CaCu_2O_{8.23}$ (0.23 holes per CuO_4 unit), (d) calculated Cu 2*p* spectrum for the Cu_3O_{10} cluster with four holes (0.33 holes per CuO_4 unit).

Recently we have proposed[13,14] that these questions can be resolved by model calculations that go beyond the Anderson impurity limit. For the description we will use a Cu_3O_{10} cluster (see the inset in the upper part of Fig. 1). The cluster consists of a reduced basis set of Cu $3d_{x^2-y^2}$ orbitals and the σ-bonding O 2*p* orbitals. This basis set gives an adequate description of the Cu 2*p* spectrum, since in core-level photoelectron spectroscopy the number of valence electrons is unchanged.[14] Besides that, it will also provide a description of the IPES spectrum as we will show in the next section.

The Hamiltonian includes a one-particle part describing the hybridization between nearest-neighbor Cu $3d_{x^2-y^2}$ and O 2*p* orbitals given by the Slater Koster[15] integral $pd\sigma$, and the hopping between nearest-neighbor O 2*p* orbitals, given by $pp\sigma$ and $pp\pi$. The two-particle part of the Hamiltonian describes the interaction between two holes on the same Cu site, with $U_{x^2-y^2\uparrow,x^2-y^2\downarrow} = A + 4B + 3C$ in terms of Racah parameters, and the Coulomb interaction between two holes on the same oxygen orbital, described by U_{pp}. Introducing a core hole on the central Cu site will lead to a Coulomb interaction between the core hole and the valence holes (the consequences of the multiplet effects in this interaction will be discussed later). The parameters used in these calculations (see Table II) are also suitable for explaining the valence-band spectra and agree well with the values obtained from constrained local-density approximation (LDA) calculations.[16,17]

The spectrum with three holes (undoped) is shown in Fig. 1(b). Note the wide asymmetric shape of the main line. It turns out[14] that the main line has two different contributions. The lowest final state does not have mainly $\underline{c}3d^{10}\underline{L}$ character as would be expected in the Anderson impurity limit, but a $\underline{c}3d^{10}$ character. The hole has moved to a neighboring CuO_4 unit thereby forming a Zhang-Rice singlet[2] with mainly $3d^9\underline{L}$ character in a $^1A_1$ symmetry.[3] This situation is energetically more favorable than the $\underline{c}3d^{10}\underline{L}$ configuration as a result of the small benefit from hybridization in the latter situation caused by the strong core-hole potential, compared to the large

TABLE II. Parameters used in the calculations for the Cu_3O_{10} cluster with a reduced basis set and those for the calculation including multiplet effects and $2p$ spin-orbit coupling using a Cu_5O_{16} cluster (see also Refs. 10 and 18).

	Cu_3O_{10}	Cu_5O_{16}
$\varepsilon_p-\varepsilon_d$	3.5	3.5
$pd\sigma$	1.5	1.5
$pd\pi$		−1.0
$pp\sigma$	−1.0	−1.0
$pp\pi$	0.3	0.3
$10Dq$		0.3
A	6.6	6.6
B	0.15	0.15
C	0.60	0.60
U_{pp}	6.0	6.0
F^0_{pd}	7.7	8.0
F^2_{pd}		7.47
G^1_{pd}		5.62
G^3_{pd}		3.20
ζ_p		13.6

stabilization energy of the Zhang-Rice singlet. The $\underline{c}3d^{10}\underline{L}$ state therefore appears at a higher binding energy in the main line. The satellite is a result of the finite overlap of the ground state with a core hole removed with the unscreened final state, and has mainly $\underline{c}3d^9$ character.

Experimentally, for $Bi_2Sr_2Ca_{1-x}Y_xCu_2O_{8+\delta}$ a broadening of the main line is observed as a function of doping. Compare, for example, the insulating sample $Bi_2Sr_2YCu_2O_{8.51}$, with 0.01 holes per CuO_2, with the hole-doped sample $Bi_2Sr_2CaCu_2O_{8.23}$, with 0.23 holes per CuO_2, in Figs. 1(a) and 1(c), respectively. Similar behavior is also found for the calculation for the Cu_3O_{10} cluster when going from 3 to 4 holes, see Fig. 1(d). Furthermore, in going from the undoped to the approximately 33% doped system, the satellite to main intensity ratio hardly changes, which is also found experimentally for the Bi series where the intensity ratio of the satellite and main peak has a value of 0.37 ± 0.1 for x ranging from 0.0 to 1.0.[6]

Up to now we have a poor agreement between the theoretical and experimental satellite structure. This is a consequence of the fact that all the multiplet effects of the $2p$-$3d$ Coulomb interaction and the spin-orbit interaction have been neglected. The inclusion, however, requires that all the $3d$ orbitals, on the site where the core hole is created, plus all the oxygen ligands of the same symmetry are taken into account. One also has to consider all spin degrees of freedom and include explicitly the $2p$ hole instead of treating it as a simple core-hole potential. All these aspects increase the size of the problem and made, e.g., the calculation for the Cu_3O_{10} cluster with all valence holes no longer possible. In a previous paper,[13] where we considered the Ni $2p$ XPS spectrum, this problem was solved by "freezing" the valence holes of the metal atoms, other than the one where the core hole is created, onto the metal atom. The loss in hybridization energy can then be compensated by adjusting the $3d$ orbital energy ε_d in such a way that the energy needed to add a hole to the CuO_4 unit with a frozen hole is equal to the energy difference between a cluster with two holes (i.e., with a Zhang-Rice singlet) and one with one hole. Although this worked well for NiO, for CuO and the high-T_c compounds the larger covalency leads to a stronger decrease in the Cu $3d$ hole count as a result of the spreading of the wave function to neighboring Cu sites. To avoid this problem, which affects the Cu $2p$ XPS spectrum, the orbital energies of the other Cu atoms are raised to a higher energy for the ground state and only play a role in the final state where they are essential for the nonlocal screening. The good agreement between a calculation for the Cu_3O_{10} cluster with three holes and a calculation for the same cluster (without multiplet effects and the spin-orbit interaction), using this approximation, seems to justify this procedure.

The calculation including multiplet effects and the spin-orbit interaction has been done for a Cu_5O_{16} cluster, where the copper atom on which the core electron is removed is surrounded by four CuO_4 clusters (see, the schematic picture in Fig. 2). The values for the U_{pd} Coulomb parameters are the same as those used by Okada and Kotani.[18] The radial parts of the pd Coulomb interaction F^2_{pd}, G^1_{pd}, and G^3_{pd} have been calculated within the Hartree-Fock limit,[19] and are renormalized to 85% of their bare value to account for screening effects. The value of the $2p$ spin-orbit coupling energy has been taken to be 13.6 eV whereas the $3d$ spin-orbit coupling has been set to zero. The Cu $2p$ spectrum is shown in Fig. 2. To obtain a better agreement with the experimental satellite structure a small crystal field of 0.3 eV has been introduced.

The first thing we observe is that the change from a Cu_3O_{10} to a Cu_5O_{16} cluster leads to a wider main line. This is to be expected since adding two CuO_4 units to the Cu atom, where the $2p$ electron is removed, leads to a larger effective hybridization between the configurations with the hole on the central CuO_4 unit (i.e., the one with the core hole) and those with the hole on a CuO_4 unit neighboring the Cu atom with the core hole. Second, we note that there is a substantial difference between the Cu $2p^{3/2}$ and the $2p^{1/2}$. The intensity difference is caused by the fact that the multiplicity of $j=\frac{3}{2}$ is twice that of

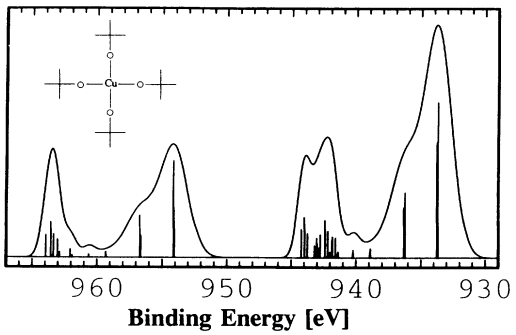

FIG. 2. Calculated Cu $2p$ spectrum including multiplet effects and $2p$ spin-orbit coupling for a Cu_5O_{16} cluster (shown schematically in the figure).

$j=\frac{1}{2}$. The multiplet effects do not give rise to a large difference in shape for the main line but strongly affects the satellite shape. The satellite of $2p^{3/2}$ has the well-known squarish shape, whereas that of Cu $2p^{1/2}$ is much narrower. Similar effects are also observed experimentally.[7] In contrast to the shape, the satellite-to-main-intensity ratio is hardly affected by the multiplet part of the *pd*-Coulomb interaction. The ratios are 0.39 and 0.41 for the Cu $2p^{1/2}$ and $2p^{3/2}$, respectively.

IV. EFFECTS OF DOPING ON LOW-ENERGY STATES

As a function of doping one observes some very important phenomena. When the antiferromagnetic insulator is doped with holes or electrons it becomes metallic and superconducting with a critical temperature dependent on the number of holes in the CuO_2 planes (see, e.g., for $Bi_2Sr_2Ca_{1-x}Y_xCu_2O_{8+\delta}$, Table I). During an insulator-metal transition, states will have to appear at the Fermi level, which is also clearly observed in most high-T_c compounds. This leaves the question of where these states originate from. An effect accompanying the growth of intensity near the Fermi level is the disappearance of intensity at higher energies above the Fermi level. This effect is most clearly observed in x-ray absorption spectroscopy (XAS) (Refs. 20 and 21) and electron-energy-loss spectroscopy (EELS) (Ref. 22) data. This phenomenon is clearly a many-body effect. Since in an independent electron model the energy bands are only weakly dependent upon filling (assuming that the Hamiltonian does not severely change upon doping, e.g., by the introduction of impurity potentials) it is very hard to describe a transfer of spectral weight, considering that the weight of a state is always 1. However, in a strongly correlated electron model one is dealing with combinations of Slater determinants and therefore the spectral weights can be smaller than one and also strongly doping dependent and we could thus expect the doping to cause transfer of spectral weights.

The explanations of the consequences of doping the antiferromagnetic insulator can be roughly divided into two groups. In both cases the starting point is the half-filled insulator with the chemical potential in the middle of the gap [see Fig. 3(a)]. In the first explanation *the chemical potential stays fixed and energy states move towards the Fermi level* to form the so-called "midgap"states[23,24] [see Fig. 3(b)]. In this case the hole will thus not move into the lowest electron removal eigenstate of the insulator, but into newly formed states.

A second explanation for the appearance of intensity near the Fermi level is that the *chemical potential shifts* towards the valence (conduction) band to accommodate the extra holes (electrons). Many-body effects now cause a *transfer of spectral weight* from the upper (Hubbard) band to the lower [see Fig. 3(c)]. Experimentally it is very difficult, if not impossible, to distinguish between a shift of states and a transfer of spectral weight, hence the importance of determining the effect of doping on the position of the chemical potential. In the remainder of the paper we will discuss our data on the

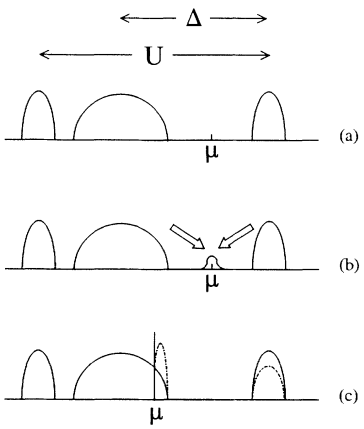

FIG. 3. Schematic picture of the proposed effects of doping on the electronic structure. For the antiferromagnetic insulator the chemical potential is in the middle of the gap; see (a). The consequences of doping can be divided into two groups: the chemical potential stays fixed and states move towards the chemical potential—see (b)—or the chemical potential moves to the top of the valence band and strong correlation effects cause a transfer of spectral weight (dashed line); see (c).

$Bi_2Sr_2Ca_{1-x}Y_xCu_2O_{8+\delta}$ series and show that they are in agreement with the latter explanation.

Figure 4 shows the valence band of $Bi_2Sr_2YCu_2O_{8.51}$ and $Bi_2Sr_2CaCu_2O_{8.23}$ measured with XPS (for the valence-band spectra for the other x values see Ref. 6). For high photon energies, where there is little emission from oxygen, the general structure of the valence band can be well understood by cluster type[10] calculations or impurity calculations.[3,16] The high-T_c compounds are in the charge transfer regime of the Zaanen-Sawatzky-Allen diagram,[1] which means that the energy to transfer an electron from the ligand to the copper Δ is smaller than the Coulomb repulsion between two holes on copper U. This implies that the Cu $3d^8$ states appear at higher binding energies and that the large valence-band feature is of

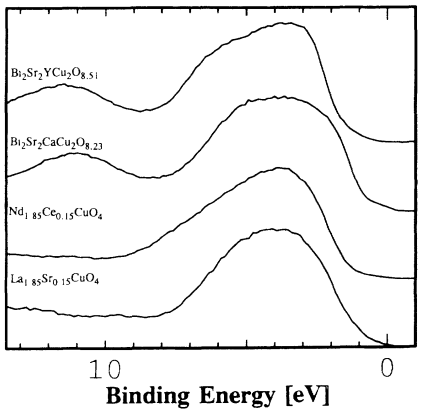

FIG. 4. Valence-band XPS spectra of (from top to bottom) and $Bi_2Sr_2YCu_2O_{8.51}$, $Bi_2Sr_2CaCu_2O_{8.23}$, $Nd_{1.85}Ce_{0.51}CuO_4$, and $La_{1.85}Sr_{0.15}CuO_4$.

mainly $3d^9\underline{L}$ character, where $\underline{L}$ stands for a hole on the oxygen ligands. But, since in the high-T_c the CuO_2 planes are strongly covalent, the main valence-band feature has besides a large $3d^9\underline{L}$ contribution also a considerable amount of d^8 and $d^{10}\underline{L}^2$ character. The feature between 10 and 13 eV in the Bi-based high-T_c compounds should probably be attributed to Bi 6*s* states. Although the satellite is quite often not visible it shows a clear resonance near the Cu 3*p* binding energy.[12,23]

Previously, Allen *et al.*[23] drew conclusions about the pinning of the Fermi level by comparing hole-doped $La_{2-x}Sr_xCuO_4$ with the electron-doped compound $Nd_{2-x}Ce_xCuO_4$. Comparing two different compounds should always be done with the upmost care since there is always the uncertainty whether one is comparing the same spectral features. Consider, for example, the valence-band spectra of $Nd_{1.85}Ce_{0.15}CuO_4$ and $La_{1.85}Sr_{0.15}CuO_4$ (see Fig. 4). Similar samples were previously studied by Namatame and co-workers.[25] The $La_{1.85}Sr_{0.15}CuO_4$ was a single crystal, the $Nd_{1.85}Sr_{0.15}CuO_4$ a reduced sintered pellet. Both samples were scraped in vacuum to obtain a clean surface.

The spectra all have a different shape, even the two $Bi_2Sr_2Ca_{1-x}Y_xCu_2O_{8+\delta}$ compounds. These dissimilarities could be caused by a number of reasons. First of all, there is a difference in crystal structure. To a first approximation all the samples can be described by a single CuO_4 unit and one would therefore expect a similar valence-band structure. However, looking at the next layer of oxygens neighbors we see that for the $Bi_2Sr_2Ca_{1-x}Y_xCu_2O_{8+\delta}$ samples there is actually a fivefold oxygen surrounding. $La_{2-x}Sr_xCuO_4$, which has the K_2NiF_4-T structure, has elongated CuO_6 octahedra, while for $Nd_{2-x}Ce_xCuO_4$, which has the same crystal structure, although it is now the T′ phase, there are eight nearest-neighbor oxygens, but at a larger distance. Especially when comparing details of the spectra of different compounds, like the onset of the large valence band feature, these differences cannot be neglected.

Second, the photoemission spectra of a doped system are not equivalent to that of the insulator. This is already apparent from the differences between the two end species of one compound, $Bi_2Sr_2YCu_2O_{8.51}$ and $Bi_2Sr_2CaCu_2O_{8.23}$. The presence of Zhang-Rice singlets (or $3d^{10}$ configurations for the Nd-Ce-Cu-O compound) can lead to different spectra as was shown by Eskes and Sawatzky who performed calculations of the doping dependence of the valence-band spectra of a Cu_2O_7 cluster.[10] Due to the change in valence-band structure by different crystal structures and doping effects it becomes necessary to include in a study on the behavior of the chemical potential not only the valence band, but also the major core levels since they would immediately follow a shift of the chemical potential.

In a previous paper[6] we reported the main results of our XPS data on the $Bi_2Sr_2Ca_{1-x}Y_xCu_2O_{8+\delta}$ system. The conclusion was that the chemical potential shifts in a manner consistent with that of a simple doped semiconductor. These shifts of the core levels have also been interpreted in terms of changing effects[26] or chemical shifts.[27] The first possibility always remains a difficult point, but from data taken with different x-ray beam intensities we estimate the charging effects to be less than 0.1 eV for the insulating sample. Another point is that the shift of the Bi 4*f* level is about half that of all the other major core levels, which is very hard to explain if one assumes charging effects to be the dominant factor for these shifts, since in that case all the core levels would give a uniform shift. The deviant behavior of the Bi 4*f* level should probably be attributed to the fact that the extra oxygen is incorporated in the Bi_2O_2 planes.[4] Itti *et al.*[27] interpreted the measured shifts by chemical shifts. Therefore, upon doping the system with holes, e.g., the copper and oxygen binding energies would have to continue the trend when going from Cu_2O to CuO, which also follows from the calculations by Itti *et al.*, using bond valence sums. On going from a formal copper valency +1 to +2 the O 1*s* core level shifts to a lower binding energy. We see that a further increase of the copper valency in the high-T_c compounds indeed leads to a lowering of the binding energy. For the Cu 2*p* level, however, Itti *et al.*[27] calculated an increase in the binding energy upon hole doping, in agreement with the expected change in binding energy continuing the behavior when going from Cu_2O to CuO. However, experiment shows just the opposite, namely, a shift to lower binding, like the O 1*s* level.

Therefore, we believe that, regarding the similar behavior of the valence band and the major core levels, a shift of the chemical potential is the most logical explanation for our data. The changes in binding energy due to different Madelung potentials, bond lengths, etc., all of which can shift the binding energy in either direction, are estimated to be less than 0.1 eV. From our data we can distinguish two different regimes. On going from the insulator to the metal,[4] $1.0 \leq x < 0.6$, we first observe a rapid shift of approximately 0.5 eV. This is followed by a slow shift of the chemical potential for the metallic compounds. The first part can be identified as a shift of the chemical potential from a position in the gap to a position at the top of the valence band. By the top of the valence band we mean the part of the spectrum between 0 and 1 eV in front of the large valence-band feature (see Fig. 4). The second part is interpreted as a gradual shifting of the chemical potential through the valence band. Assuming a rectangular band with one electron per state one can estimate that for these shifts a bandwidth of 1 eV is necessary to explain the differences in hole density.

This behavior of the chemical potential upon doping is very similar to that of the Hubbard system, as calculated by Dagotto *et al.*[28] using Lanczos techniques. They observe a rapid shift of half the insulating gap at the metal insulator transition, corresponding to a shift of the chemical potential in the center of the gap to the top of the lower Hubbard band (or the bottom of the upper Hubbard band for electron doping, which is equivalent due to the electron-hole symmetry). This is then followed by a slower shift through the lower Hubbard band during which electrons are being gradually removed from the lattice.

Figure 5 shows the UPS and IPES spectra for the $x=0.0$, 0.3, 0.5, 0.75, and 1.0 samples. For the insulator without calcium it was impossible to obtain a well-focused electron beam, which made it impossible to obtain a good IPES spectrum. The incoming electron energy is 18.7 eV. The UPS spectra have been normalized to the area of the main valence-band feature, the IPS measurements to the maximum of the peak at 4 eV. At He I energy the cross section of oxygen is about twice as large as for copper. Therefore, there is a substantial contribution from oxygen features to the valence band, i.e., from BiO, CuO, and SrO bands. Also, with UPS, a shift of the chemical potential towards the valence band can be observed (note, for example, the shift of the maximum of the valence band). The spectra also show a disappearance of states at approximately 3 eV and there is a new shoulder appearing at 1.2 eV for the $x=0.0$ compound. Also in their angle resolved ultraviolet photoemission (ARUPS) data, Takahashi *et al.*[29] find a band that shifts from 2.4 to 1.5 eV when comparing the $x=0.6$ and 0.0 compounds of $Bi_2Sr_2Ca_{1-x}Y_xCu_2O_{8+\delta}$ single crystals. This is larger than would be expected from the chemical potential shift, which is 0.2–0.3 eV in this region. The origin of this effect is still unclear.

The most significant changes occur near the Fermi level. This part has been blown up 20 times in Fig. 5. On going from the 100% to the 0% doped sample we observe a number of changes: first, the onset of the large valence band at 1.5 eV feature shifts towards the Fermi level when the system is doped with holes; second, a bandlike feature gradually appears out of the large onsets; third, the slope of the region nearest to the Fermi level increases with the hole density, until the cutoff is as sharp as the Ag reference (not shown) for the $x=0.0$ compound. This behavior is also observed for the $YBa_2Cu_3O_x$ series,[30] but also for electron-doped $Nd_{2-x}Ce_xCuO_4$.[31,32] So far this latter effect is in contrast with calculations on the Hubbard system, where the intensity is usually highest near the chemical potential.

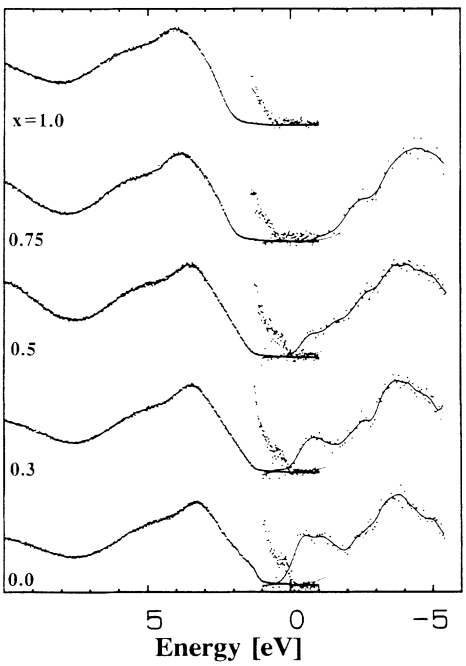

FIG. 5. UPS ($\hbar\omega=21.2$ eV) and IPES (with an incoming electron energy of 18.7 eV) of $Bi_2Sr_2Ca_{1-x}Y_xCu_2O_{8+\delta}$ with from top to bottom $x=1.0$, 0.75, 0.5, 0.3, and 0.0. The region near the Fermi level of the photoemission spectra has been multiplied 20 times.

From the $x=0.75$ sample we see that the gap for the insulator is approximately 2 eV. Hereby the onset of the high-energy band in the IPES spectrum, corresponding to the $3d^{10}$ levels, has been taken as the lowest $N+1$ eigenstate for the insulator. The fact that the gap on the UPS side is 0.5 eV for the $x=0.0$ insulator implies that the chemical potential is not in the center of the insulating gap. This is not surprising since even in the sample with 100% yttrium there is a hole density of approximately 0.01 per CuO_2 unit. And, as already mentioned in the discussion of the shift of the chemical potential, a small number of holes can already shift the chemical potential by an amount of the order of half the gap value. There is, however, a remarkable discrepancy between the real high-T_c compounds and the model systems, e.g., the different Hubbard models, namely, that in the latter the metal-insulator transition always occurs at half-filling, whereas the former remain semiconductors up to relatively high doping levels, approximately 0.08 holes per CuO_2 unit. So far this has only been explained by the introduction of small impurity potentials, that bind the holes (electrons) up to a certain doping level where the impurity states start forming bands, which overlap the valence band.

ARUPS (Refs. 33 and 34) and angle resolved inverse photoemission (ARIPS) (Ref. 35) have also shown band crossings giving more or less the same Fermi surface topology as predicted by band structure calculations for both hole- and electron-doped materials. This shows that there is a large Fermi surface that is consistent in size with the number of electrons and not with the number of dopants to the half-filled insulator. This seems to exclude the existence of hole pockets. Also these band crossings at particular k values make it less probable that these states are a result of impurities.[36] It should be noted that for systems which can be viewed to first order as an effective hopping between sites the electron removal and addition spectral functions usually also lead to a tight-binding-like dispersion relation. See, for example, the spectral functions of the t,J model or the three-band Hubbard model.[37] Therefore, the Fermi level crossings usually merely reflect the structure of the underlying lattice and electron filling and cannot be viewed as a justification of independent electron approaches or a Fermi-liquid description.

A much better indication for the degree of correlation is the dispersional width of the "bands" crossing the Fermi level. Here we see that the bandwidths of 0.5–1 eV, as determined by ARUPS (Refs. 33 and 34) and ARIPS (Ref. 35) or by the shift of the chemical potential upon doping, are strongly renormalized with respect to the local-density approximation band-structure calculations (although there is still some discrepancy[31,32] whether this is also the case for electron doped $Nd_{2-x}Ce_xCuO_4$). Cal-

culations on model Hamiltonians of correlated systems also lead to strong renormalizations of the bandwidth compared to the single electron transfer integral.[37] This is because the effective particles are no longer independent electrons, but, e.g., the singlets in the t,J model, the Zhang-Rice singlets[2,3] in the three-band Hubbard model, or other highly dressed particles.

The validity of the independent (quasi)particle approach for the high-T_c still remains uncertain. On the one hand, theoretically, since experimental data, like transport measurements, are very hard to reconcile with a Fermi-liquid picture.[38] On the other hand, experimentally, where, if the Fermi-liquid picture were valid, one should observe a sharp peak[39] well separated from the background (the incoherent part of the Green's function) very close to the Fermi level. The resolution, however, is not sufficient to draw any definite conclusions.

So far, from a spectroscopic point of view, a number of features point towards a breakdown of the Fermi-liquid picture. One of the first things that was pointed out was the fact that the structure of the valence band can only be interpreted by including strong correlations. Especially important for the recognition of this was the Cu d^8 satellite at roughly 13 eV, which shows a resonance at the Cu $3p$ binding energy, i.e., around 74 eV. This clearly indicates the presence of strong correlations between holes on a copper site. Second point is the strong reduction of the bandwidths not only near the Fermi level, but also at higher binding energies. A third point is the transfer of spectral weight from high- to low-energy states in the electron addition spectra, which can only be understood in many-body terms. This will be discussed in the next paragraph.

V. TRANSFER OF SPECTRAL WEIGHT

In the inverse-photoemission spectra there is a clear increase of states near the chemical potential when the density of holes per CuO_2 unit is increased by substituting Y by Ca in $Bi_2Sr_2YCu_2O_{8.51}$. At first sight it looks like the inverse photoemission can be most easily explained by the appearance of new states at a fixed Fermi level. Similar conclusions were also drawn by Matsuyama *et al.*[36] on basis of their XAS data (they interpreted these states as impurity states). However, we believe that these data can also be interpreted in a different way. Namely, by a shift of the chemical potential combined with a transfer of spectral weight. There are a number of reasons for doing so. In the previous section (see also our paper on the XPS spectra[6]) we have shown that there is a clear shift of the chemical potential, indicating that the chemical potential moves to the top of the valence band. Another point is that it is very reasonable to expect that the effects of hole doping can be described in more or less similar terms for all high-T_c superconductors. Other compounds show very clearly, besides the appearance of spectral weight at the chemical potential, a decrease in intensity at an energy about 2 eV higher. In the Bi series these high-energy states are for some reason much less pronounced. In our IPES spectra we observe a decrease in intensity around 2.4 eV. To elucidate this transfer of spectral weight the intensity coming from the peak around 4 eV, which should be attributed to BiO states has been removed [see Fig. 6(d)]. This was done by subtracting a Gaussian with a height equal to the maximum of the peak and a width of 2.9 eV. This Gaussian was subsequently matched to the spectrum at 3 eV (see the thin lines in Fig. 5). This transfer of spectral weight is analogous to that observed in $La_{2-x}Sr_xCuO_4$ and $YBa_2Cu_3O_x$ in both XAS (Refs. 20 and 21) and EELS (Ref. 22) measurements, although it is much clearer.

This transfer of spectral weight is most easily explained by making use of the one-band Hubbard description of the high-T_c compounds.[40–42] When adding an electron to the half-filled insulator, the final state will always have a doubly occupied site. The electron addition spectrum will thus only show an upper Hubbard band. After doping this situation will drastically change. Without hybridization the effect of removing an electron from the system will be that at a particular site there are two possibilities of reaching a final state with one electron on each site, while for the remaining sites the situation is unchanged from the insulator. Since in the former situation both electrons will end up in the lower Hubbard band, because there are no doubly occupied sites, the lower Hubbard band has gained twice as much intensity as the upper Hubbard band has lost. Thus, the low-energy spectral weight grows as $2x$ instead of x as would be expected for a rigid band picture.[40,42]

Upon switching on the hybridization there is another

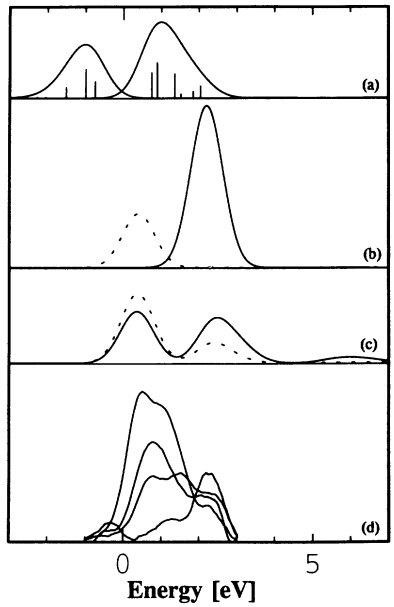

FIG. 6. (a) Photoemission and inverse photoemission spectra for a Cu_3O_{10} cluster with three holes, (b) inverse-photoemission spectrum for the Cu_3O_{10} cluster with four holes with the hybridization between copper and oxygen $pd\sigma$ equal to zero, (c) inverse-photoemission spectrum for the Cu_3O_{10} cluster with $pd\sigma = 1.5$ eV [in (b) and (c) the solid and dashed lines show the Cu $3d$ and O $2p$ electron addition, respectively], and (d) transfer of spectral weight for the $Bi_2Sr_2Ca_{1-x}Y_xCu_2O_{8+\delta}$ with $x = 0.75$, 0.5, 0.3, and 0.0. The spectra are those of Fig. 5 after a background correction (see the thin line in Fig. 5).

hybridization channel to the lower Hubbard band via the hopping matrix the so-called kinetic effect.[40,43] This effect depends on the hole concentration and has a magnitude proportional to, in first order, t/U, where t is the transfer integral and U the on-site repulsion between two electrons. This can be understood in a qualitative way. First the electron has to end up in an already occupied site. The chance for this is proportional to $1-x$, where x is the hole density away from half-filling. In order to reach the lower Hubbard band the pair has to be broken, hence the $1/U$, and the electron has to jump to an empty neighboring site, which gives the t. The probability of the last process is proportional to the hole density x. In this very simplified picture the extra contribution to the transfer of spectral weight is parabolic $\sim t(1-x)x/U$, with a maximum at a quarter filling [in fact the behavior turns out to be sinusoidal to first order, $4|t|\sin(x\pi)/\pi U$, which follows from the expectation value $\langle c^{+}_{i-\sigma}c_{j-\sigma}\rangle$, which is related to the kinetic energy[43]]. Exact diagonalization for small clusters shows that this maximum shifts to higher electron densities.[41]

For a charge-transfer compound the situation is more complicated, due to the presence of the oxygen band. The behavior of the chemical potential and the IPES spectrum upon hole doping can also be simulated with the Cu_3O_{10} cluster. In the undoped case the chemical potential is in the middle of the PES-IPES gap [see Fig. 6(a)]. Let us first consider the case with the hybridization between copper and oxygen $pd\sigma$ zero [see Fig. 6(b)]. For the case of four holes, three will go onto the Cu atoms and one into the oxygen band as a result of the strong repulsion between two holes on one Cu atom. The IPES spectrum will therefore show a 3:1 intensity ratio between the Cu $3d$ and O $2p$ electron addition spectral functions. Thus the chemical potential in the ionic situation shifts through the oxygen bands (with the $3d^{10}$ states moving away from the chemical potential) and the intensity of the lower band in IPES would be just proportional to the number of doped holes. However, this is not what is found experimentally where the lower band grows much faster than might be expected from a rigid band behavior [see Fig. 6(d)].

Upon switching on the hybridization in the Cu_3O_{10} cluster a similar behavior is observed. The peak at higher energies, corresponding to the states with a mainly $3d^{10}$ character (i.e., the Hubbard band) shows a strong decrease with its spectral weight predominantly transferred to the low-energy states. This can be understood as follows. The doped holes have their largest weight on oxygen and due to hybridization effects they form the so-called Zhang-Rice singlets,[2] which have a $^1A_1$ symmetry.[3] In an ionic picture these states can be described as $d^9\underline{L}$. The low-energy inverse photoemission states are of d^9 character and can therefore only be reached by adding an electron at an oxygen site. Upon switching on the hybridization this picture changes. The low-energy final states also now have a substantial $d^{10}\underline{L}$ contribution, which can also be reached by adding a d electron to a Zhang-Rice singlet. While for the low-energy bands these two contributions add, for the high-energy states this interference works destructively (the extra $d^{10}\underline{L}^2$ and $3d^8$ character of the Zhang-Rice singlet due to the hybridization only further decreases the intensity of the high-energy states). Already for a t_{pd}/U ratio of 0.25, with t_{pd} the copper oxygen hybridization, the similarities with the one-band Hubbard model are already quite large, i.e., for every added hole the low-energy states grow twice as fast as the high-energy states decrease.[40]

It is unclear why the intensity of the high-energy band is so much less pronounced in the $Bi_2Sr_2Ca_{1-x}Y_xCu_2O_{8+\delta}$ compounds compared to other high-T_c materials. So far, to our knowledge, it has not been observed in either XAS (Ref. 36) or EELS (Ref. 22), nor in IPES (Ref. 44). Also, in these IPES measurements, this effect is already obscured at higher incoming electron energies due to the lower cross section of these states and due to the lesser resolution of the IPES spectrometer [see Fig. 7]. Due to the absence of clear transfer of spectral weight the states near the Fermi level have also been interpreted as impurity bands or doping induced "midgap" states. Since the major difference between the La-Sr-Cu-O, the Y-Ba-Cu-O compounds and $Bi_2Sr_2Ca_{1-x}Y_xCu_2O_{8+\delta}$ is the presence of other bands (of a mainly Bi-O character) at the same energy as the high-energy electron addition states a possible explanation might be that hybridization with those features spreads out the upper Hubbard band.

Another deviant aspect in the data for the Bi-series is the filling in of the region between the low-energy states and the upper Hubbard band. This result is also known from exact diagonalization of the Hubbard system for small clusters. For the half-filled system there are no

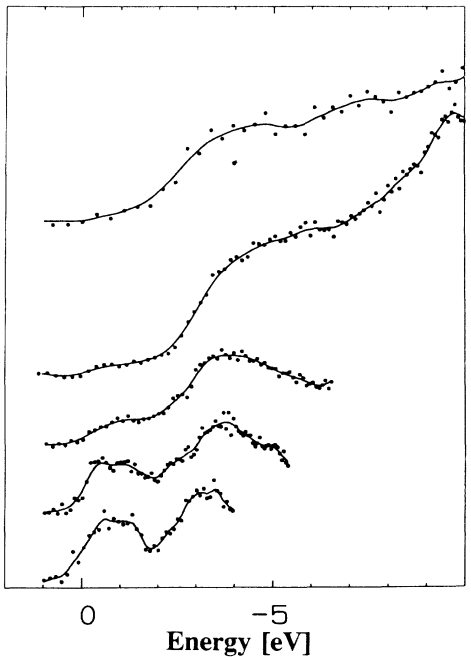

FIG. 7. Inverse-photoemission spectra of $Bi_2Sr_2CaCu_2O_{8.23}$ for different incoming electron energies. From top to bottom $E_k = 30.7$, 26.7, 22.7, 18.7, and 16.7 eV. The resolution decreases from 0.3 eV at low photon energies to 1.0 eV at high photon energies.

states in the gap. However, after doping the gap region can fill since, e.g., by adding an electron to the $N-1$ system one can also reach excited states of the N system. For the Hubbard system these effects are only visible for large hybridization strengths. However, one can also think of other excitations of the highly dressed effective particles, like polaronic effects, magnons, etc., which are not included in the Hubbard model. (A nice analogy is the H_2 molecule where one can observe after electron removal a large number of excited vibronic states as a result of the finite Franck-Condon factors.[39])

Figure 7 shows IPS spectra on $Bi_2Sr_2CaCuO_{8.23}$ for several different incident electron energies from 16.7 to 30.7 eV. The observed features are in agreement with previously published measurements on $Bi_2Sr_{2-x}Ca_xCu_2O_8$.[45] The intensity of the states closest to the Fermi level slowly decreases, which is in correspondence with the fact that they have largely an oxygen character. The broad feature from 2 to 6 eV should be attributed to Bi $6p$ states and the peak at 9.5 eV from empty Ca $3d$ levels. The increased intensity of this level at an incoming electron energy of 26.7 eV is a result of interference with the radiative decay of a plasmon with an energy of 15 eV.[45]

VI. DISCUSSION

In this paper we have presented evidence against the theories that claim that the introduction of holes into the insulator creates new states at the chemical potential; instead that the increase of intensity near the chemical potential is caused by a shift of the chemical potential through the valence band, combined with a transfer of spectral weight from the high-energy states to these low-energy states. This is in agreement with quantum Monte Carlo calculations and exact diagonalizations of Hubbard-like models. Note that such a transfer cannot be described by a t-J model or other models where the high-energy states have been projected out. Eskes, Meinders, and Sawatzky[40,41] have shown that this spectral weight transfer strongly depends on the density of doped holes or electrons. Therefore, this effect might be of crucial importance when describing phenomena that involve density fluctuations. A decoupling of the low- and high-energy states might then no longer be possible. This is in sharp contrast with Fermi-liquid theories, where a change of the high-energy physics only leads to a renormalization of the constants needed to describe the low-energy physics. Another possible description using only the low-energy states would have to take into account that the available phase space for the low-energy states does not change by one when an electron is removed from the system but by a large number.

The experimental facts pointed out in this paper, a shift in the chemical potential and a transfer of spectral weight as a function of doping, can be found in most high-T_c compounds. The transfer of spectral weight is very clear in XAS and EELS for $La_{2-x}Sr_xCuO_4$ (Refs. 20 and 21) and $YBa_2Cu_3O_x$ (Refs. 21 and 22) and has now also been found in $Bi_2Sr_2Ca_{1-x}Y_xCu_2O_{8+\delta}$. The electron-doped $Nd_{2-x}Ce_xCuO_4$ series still remains a point of controversy. Anderson *et al.*[31,32] recently shown an apparent absent of a shift of the chemical potential to the conduction band, which they concluded from the fact that the gap on the PES side is 0.5 eV, whereas the total gap is supposed to be 1.5 eV.

The combination of a chemical potential shift with a transfer of spectral weight is also not a unique aspect of the high-T_c compounds. It is also apparent in a number of doped late transition metal oxides. For a large number of these systems the extra hole sits on the oxygen (they are in the charge transfer or the intermediate regime of the Zaanen-Sawatzky-Allen diagram[1]), like the high-T_c compounds. One of the simplest doping mechanisms is replacing the transition metal by lithium or sodium. The transfer of spectral weight and also the chemical potential shift is obvious for $Li_xCo_{1-x}O$ (Ref. 46) and most notably for $Li_xNi_{1-x}O$.[47,48] Similar behavior can also be observed in the perovskites $La_{1-x}Sr_xTMO_3$ (TM = Mn, Fe, Co).[49] A very interesting case is $La_{2-x}Sr_xNiO_4$, studied by Eisaki *et al.*[50] and Kuiper *et al.*,[51] due to similarities in crystal structure with $La_{2-x}Sr_xCuO_4$ (though this compound is less two dimensional than the superconductor). It shows the chemical potential shift and, though not very clear, a transfer of spectral weight. A remarkable difference is that while $La_{2-x}Sr_xCuO_4$ becomes metallic and superconducting for $x>0.04$ the nickel compound remains semiconducting up to $x=0.8$.

Thus a spectral weight transfer and a shift of the chemical potential in a semiconductorlike way seem to be the dominant effect as a function of doping, for the high-T_c compounds as well as a number of other compounds, where electron correlation plays an important role. Both effects are also present in the Hubbard models. Also, the smaller shift of the chemical potential for the metallic compounds, compared to what one would expect from band-structure calculations, can be understood from the renormalizations of the bandwidths due to strong correlations. These models, however, fail to describe the insulating nature up to higher doping levels and the slow increase in intensity near the Fermi level on the PES side.

ACKNOWLEDGMENTS

We acknowledge A. Fujimori and H. Eisaki for providing the $La_{1.85}Sr_{0.15}CuO_4$ and $Nd_{1.85}Ce_{0.15}CuO_4$ samples. This work was supported by the "Nederlandse Stichting voor Fundamenteel Onderzoek der Materie" (FOM), the "Nederlandse Stichting voor Scheikundig Onderzoek in Nederland" (SON), and the "Nederlandse organisatie voor Wetenschappelijk Onderzoek" (NWO).

[1] J. Zaanen, G. A. Sawatzky, and J. W. Allen, Phys. Rev. Lett. **55**, 418 (1985).

[2] F. C. Zhang and T. M. Rice, Phys. Rev. B **37**, 3759 (1988).

[3] H. Eskes and G. A. Sawatzky, Phys. Rev. Lett. **61**, 1415 (1988).

[4] W. A. Groen, D. M. de Leeuw, and L. F. Feiner, Physica C **165**, 55 (1990).

[5] P. D. Johnson, S. L. Hulbert, R. F. Garrett, and M. R. Howells, Rev. Sci. Instrum. **57**, 1324 (1986).

[6]M. A. van Veenendaal, R. Schlatmann, G. A. Sawatzky, and W. A. Groen, Phys. Rev. B **47**, 446 (1993).
[7]G. van de Laan, C. Westra, C. Haas, and G. A. Sawatzky, Phys. Rev. B **23**, 4369 (1981).
[8]T. Mizokawa, H. Namatame, A. Fujimori, H. Kondoh, H. Kuroda, and N. Kosugi, Phys. Rev. Lett. **67**, 1638 (1991).
[9]P. Steiner, V. Kinsinger, I. Sander, B. Siegwart, S. Hüfner, C. Politis, R. Hoppe, and H. P. Müller, Z. Phys. B **67**, 494 (1987).
[10]H. Eskes, L. H. Tjeng, and G. A. Sawatzky, Phys. Rev. B **41**, 288 (1990); H. Eskes and G. A. Sawatzky, *ibid.* **43**, 119 (1991).
[11]A. Fujimori, E. Takayama-Muromachi, Y. Uchida, and B. Okai, Phys. Rev. B **35**, 8814 (1987).
[12]Z. X. Shen, J. W. Allen, J. J. Yeh, J.-S. Kang, W. Ellis, W. Spicer, I. Lindau, M. B. Maple, Y. D. Dalichaouch, M. S. Torikachvili, J. Z. Sun, and T. H. Geballe, Phys. Rev. B **36**, 8414 (1987).
[13]M. A. van Veenendaal and G. A. Sawatzky, Phys. Rev. Lett. **70**, 2459 (1993).
[14]M. A. van Veenendaal, H. Eskes, and G. A. Sawatzky, Phys. Rev. B **47**, 11 462 (1993).
[15]J. C. Slater and G. F. Koster, Phys. Rev. **94**, 1498 (1954).
[16]A. K. McMahan, R. M. Martin, and S. Satpathy, Phys. Rev. B **38**, 6650 (1989).
[17]M. S. Hybertsen, M. Schlüter, and N. E. Christensen, Phys. Rev. B **39**, 9028 (1989).
[18]K. Okada and A. Kotani, J. Phys. Soc. Jpn. **58**, 2578 (1989).
[19]R. D. Cowan, *The Theory of Atomic Structure and Spectra* (University of California Press, Berkeley, CA, 1981).
[20]C. T. Chen, F. Sette, Y. Ma, M. S. Hybertsen, E. B. Stechel, W. M. C. Foulkes, M. Schluter, S.-W. Cheong, A. S. Cooper, L. W. Rupp, Jr., B. Batlogg, Y. L. Soo, Z. H. Ming, A. Krol, and Y. H. Kao, Phys. Rev. Lett. **66**, 104 (1991).
[21]P. Kuiper, G. Kruizinga, J. Ghijsen, M. Grioni, P. J. W. Weijs, F. M. F. de Groot, G. A. Sawatzky, H. Verweij, L. F. Feiner, and H. Petersen, Phys. Rev. B **38**, 6483 (1988); T. Takahashi, S. Suzuki, T. Kusunoki, S. Sato, H. Katayama-Yoshida, A. Yamanaka, F. Minami, and S. Takeawa, Physica C **185-189**, 1057 (1991).
[22]H. Romberg, M. Alexander, N. Nücker, P. Adelmann, and J. Fink, Phys. Rev. B **42**, 8768 (1990); J. Fink, N. Nücker, H. Romberg, M. Alexander, S. Nakai, B. Scheerer, P. Adelmann, and D. Ewert, Physica C **162-164**, 1415 (1989).
[23]J. W. Allen, C. G. Olson, M. B. Maple, J.-S. Kang, L. Z. Liu, J.-H. Park, R. O. Anderson, W. P. Ellis, J. T. Markert, Y. Dalicaouch, and R. Liu, Phys. Rev. Lett. **64**, 595 (1990).
[24]H. Matsumoto, M. Sasaki, and M. Tachiki, Solid State Commun. **71**, 829 (1989).
[25]H. Namatame, A. Fujimori, Y. Tokura, M. Nakamura, K. Yamachuchi, A. Misu, H. Matsubara, S. Suga, H. Eisaki, T. Ito, H. Takagi, and S. Uchida, Phys. Rev. B **41**, 7205 (1990); A. Fujimori, Y. Tokura, H. Eisaki, H. Takagi, S. Uchida, and E. Takayama-Muromachi, *ibid.* **42**, 325 (1990).
[26]K. Tanaka, H. Takaki, K. Koyama, and S. Noguchi, Jpn, J. Appl. Phys. **29**, 1658 (1990).
[27]R. Itti, F. Munakata, K. Ikeda, H. Yamauchi, N. Koshizuka, and S. Tanaka, Phys. Rev. B **43**, 6249 (1991).
[28]E. Dagotto, A. Moreo, F. Ortalani, J. Riera, and D. J. Scalapino, Phys. Rev. Lett. **67**, 1918 (1991).
[29]T. Takahashi, H. Matsuyama, H. Katayama-Yoshida, K. Skei, K. Kamiya, and H. Inokuchi, Physica C **170**, 416 (1990).
[30]B. W. Veal, J. Z. Liu, A. P. Paulikas, K. Vandervoort, H. Claus, J. C. Campuzano, C. Olson, A.-B. Yang, R. Liu, C. Gu, R. S. List, A. J. Arko, and B. Bartlett, Physica C **158**, 276 (1989).
[31]R. O. Anderson, R. Claessen, J. W. Allen, C. G. Olson, C. Janowitz, L. Z. Liu, J.-H. Park, M. B. Maple, Y. Dalichaouch, M. C. de Andrade, R. F. Jardin, E. A. Early, S. J. Oh, and W. P. Ellis, Phys. Rev. Lett. **70**, 3163 (1993).
[32]D. M. King, Z. X. Shen, D. S. Dessau, B. O. Wells, W. E. Spicer, A. J. Arko, D. S. Marshall, J. DiCarlo, A. G. Loeser, C. H. Park, E. R. Ratner, J. L. Peng, Z. Y. Li, and R. L. Greene, Phys. Rev. Lett. **70**, 3159 (1993).
[33]T. Takahashi, H. Masuyama, H. Katayama-Yoshida, Y. Okabe, S. Hosoya, K. Seki, H. Fujimoto, M. Sata, and H. Inokuchi, Phys. Rev. B **39**, 6636 (1989); C. G. Olson, R. Liu, D. W. Lynch, R. S. List, A. J. Arko, B. W. Veal, Y. C. Chang, P. Z. Jiang, and A. P. Paulikas, *ibid.* **42**, 381 (1990).
[34]J. C. Campuzano, G. Jennings, M. Faiz, L. Beaulaigue, B. W. Veal, J. Z. Liu, A. P. Paulikas, K. Vandervoort, and H. Claus, Phys. Rev. Lett. **64**, 2308 (1990).
[35]R. Manzke, T. Buslaps, M. Skibowski, and J. Fink, Physica C **162**, 1381 (1989).
[36]H. Matsuyama, T. Takahashi, H. Katayama-Yoshida, T. Kashiwakura, Y. Okabe, N. Kosugi, A. Yagishita, K. Tanaka, H. Fujimoto, and H. Inokuchi, Physica C **160**, 567 (1989).
[37]W. Stephan and P. Horsch, Phys. Rev. Lett. **66**, 2258 (1991); G. Dopf, J. Wagner, P. Dieterich, A. Marumatsu, and W. Hanke, *ibid.* **68**, 2082 (1992).
[38]C. M. Varma, P. B. Littlewood, S. Schmitt-Rink, E. Abrahams, and A. E. Ruckenstein, Phys. Rev. Lett. **63**, 1996 (1989).
[39]G. A Sawatzky, Nature **342**, 480 (1989).
[40]H. Eskes, M. B. J. Meinders, and G. A. Sawatzky, Phys. Rev. Lett. **67**, 1035 (1991).
[41]M. B. J. Meinders, H. Eskes, and G. A. Sawatzky, Phys. Rev. B **48**, 3916 (1993).
[42]M. S. Hybertsen, E. B. Stechel, W. M. C. Foulkes, and M. Schlüter, Phys. Rev. B **45**, 10 032 (1990).
[43]A. B. Harris and R. V. Lange, Phys. Rev. **157**, 295 (1967).
[44]T. Watanabe, T. Takahashi, S. Suzuki, and H. Katayama-Yoshida, Phys. Rev. B **44**, 5316 (1991).
[45]T. J. Wagener, Y.-J. Hu, Y. Gao, M. B. Jost, J. H. Weaver, N. D. Spencer, and K. C. Goretta, Phys. Rev. B **39**, 2928 (1989).
[46]J. van Elp, H. Eskes, P. Kuiper, and G. A. Sawatzky, Phys. Rev. B **44**, 6090 (1990).
[47]P. Kuiper, G. Kruizinga, J. Ghijsen, and G. A. Sawatzky, Phys. Rev. Lett. **62**, 221 (1989).
[48]J. van Elp, H. Eskes, P. Kuiper, and G. A. Sawatzky, Phys. Rev. B **45**, 1612 (1992).
[49]M. Abbate, F. M. F. de Groot, J. C. Fuggle, A. Fujimori, O. Strebel, F. Lopez, M. Domke, G. Kaindl, G. A. Sawatzky, M. Takano, Y. Takeda, H. Eisaki, and S. Uchida, Phys. Rev. B **46**, 4511 (1992).
[50]H. Eisaki, S. Uchida, T. Mizokawa, H. Namatame, A. Fujimori, J. van Elp, P. Kuiper, G. A. Sawatzky, S. Hosoya, and H. Katayama-Yoshida, Phys. Rev. B **45**, 12 513 (1992).
[51]P. Kuiper, J. van Elp, G. A. Sawatzky, A. Fujimori, S. Hosoya, and D. M. de Leeuw, Phys. Rev. B **44**, 4570 (1991).